

Biogenic synthesis of silver nanoparticles from thyme extract for functionalization of a bioactive glass produced from rice husk ash

M. A. Pereira^{1*}, J. E. de Oliveira¹, D. J. M. de Abreu², R. H. Piccoli³, C. S. Fonseca¹

¹Federal University of Lavras, Department of Engineering, PO Box 3037, 372000-900, Lavras, MG, Brazil

²Federal University of Lavras, Biology Department, Lavras, MG, Brazil

³Federal University of Lavras, School of Agricultural Sciences of Lavras, Lavras, MG, Brazil

Abstract

The rice husk, agro-industrial residue, stands out for having silica, the main oxide former of the bioactive glass. To avoid contamination in this biomaterial, substances with bactericidal properties, like silver can be incorporated. Thus, the objective of this work is the synthesis of silver nanoparticles to functionalize a bioactive glass synthesized from rice husk ash (BRHA). The bioglass was prepared by the sol-gel method from the rice husk ash as a silica source. Silver nanoparticles were synthesized from thyme extract with AgNO₃ and their formation was verified by UV-vis spectroscopy. The glass powder was added to this solution and its structure was evaluated by SEM-EDS, ATR-FTIR, and microbiology. The bioglass powder appeared in the form of porous agglomerates and the addition of silver altered its superficial roughness by deposition. The chemical bonds of the glass network related to bioactivity were maintained after the incorporation of the nanoparticles. Microbiological analysis by the agar diffusion test confirmed the inhibitory action of the nanoparticles for *P. aeruginosa* and *S. aureus*. Therefore, the developed material presented great potential for biomedical applications.

Keywords: silica, bioglass, antimicrobial properties, agricultural and industrial waste.

INTRODUCTION

The search for biomaterials that showed bioactivity led to the development of a material known as bioglass. Silica is its main forming oxide and, generally, it is obtained through alkoxysilane precursors, like tetraethylorthosilicate (TEOS), that are expensive [1]. In view of this, the rice husk is a lower-cost alternative source for obtaining amorphous silica, with levels greater than 90% [2]. According to CONAB (2021), the 2021/22 Brazilian rice harvest was 11.5 million tons, generating a large volume of waste that presents slow biodegradation, due to its hard surface and high content of silicon and lignin [3, 4]. The implantation of bioglass in the human body can cause infections due to contaminations that are controlled using bactericidal substances. However, more than 70% of bacterial infections are resistant to one or more antibiotics frequently utilized to eradicate them [5]. This development of bacterial resistance resulted in the search for new materials with a bactericidal potential, such as silver nanoparticles, that present chemical stability, and catalytic, antibacterial, antiviral, antifungal, and anti-inflammatory activities [6].

For silver nanoparticle synthesis, the chemical reduction method is the most widely used, obtaining a stable colloidal solution in water or organic solvents. But, the use of reducing agents that are generally toxic and generate by-products that are not environmentally friendly are disadvantages of this method [7]. To get around this problem, green synthesis was developed using plant extracts or microorganisms as

nucleating agents for nanoparticles. Those nanoparticles obtained by biogenic routes are free from toxic contamination from by-products that bind to the nanoparticles during the synthesis, which provides biomedical applications [8]. When plant extracts are utilized, the reduction and stabilization of silver ions are achieved by combining biomolecules, like proteins, enzymes, polysaccharides, phenolics, tannins, vitamins, and terpenoids present in these extracts, which have medicinal and environmentally beneficial values [6, 7]. An example of vegetal extract that can be used is thyme extract, which also has bactericidal properties mainly attributed to the presence of carvacrol, cinnamaldehyde, thymol, geraniol, and eugenol [9]. Thymol and carvacrol are utilized in mouthwashes because the presence of the OH group in these compounds has an important role in their activities against bacteria found in the oral region [10, 11]. And one of the applications of bioactive glasses is for dental treatments, which makes it interesting to use thyme extract in the synthesis of nanoparticles that is incorporated into them. In this context, the aim of this work is the synthesis of silver nanoparticles by biogenic route from the thyme extract for the functionalization of a bioactive glass synthesized from rice husk ash.

MATERIAL AND METHODS

Synthesis of bioactive glass: the bioglass (BRHA) was produced with the composition of 50 SiO₂-25 CaO-25 Na₂O (%mol) in previous work [12], through the sol-gel process, with the use of rice husk ash (RHA) as a source of silica (SiO₂). The rice husk ash was obtained by the calcination of the rice husk treated with oxalic acid. Two precursor solutions were produced, sodium silicate (Na₂SiO₃), by

*marianeap16@gmail.com

<https://orcid.org/0000-0003-0399-8438>

mixing the source of silica with sodium hydroxide (NaOH, Êxodo Cient.) and highly acid calcium nitrate (CaNO_3 , Êxodo Cient.) by dissolution in nitric acid (HNO_3 , Êxodo Cient.). The proportions are expressed in Table I. The sol was formed by adding sodium silicate solution dropwise into highly acidic $\text{Ca}(\text{NO}_3)_2$ solution under constant stirring to avoid gel precipitation. The precursor sol turned into a gel after only 30 min. The gel was aged for 48 h at 80 °C and dried for 48 h at 150 °C. The dry gel was crushed in a porcelain mortar to form a fine powder, which was calcined at 600 °C (heating rate of 5 °C/min) for 4 h in an open alumina crucible and ambient atmosphere.

Table I - Proportions of chemical reagents to the precursor solutions of BRHA.

RHA (g)	NaOH (mL)	CaNO_3 (g)	HNO_3 (mL)
10	100	12.5	50

RHA: rice husk ash; BRHA: bioactive glass from rice husk ash.

Biogenic synthesis of silver nanoparticles: the synthesis was carried out based on a previous study [13] with adaptations. To summarize, thyme extract was produced by mixing 1.5 g of thyme in 30 mL of deionized water under heating and stirring for 20 min. The extract was filtered and, because of the evaporation, the volume (30 mL) was completed with deionized water, obtaining a solution of 5% m/v. The silver nitrate (AgNO_3 , Dynamic) was dissolved in deionized water to produce a 10 mM solution. After dissolution, 1 g of the bioactive glass powder was added to this solution. The thyme extract was poured over the silver nitrate solution with the glass powder, which remained dispersed in the solution, and instantly the solution turned dark brown, indicating the formation of nanoparticles. This mixture was left under stirring for 17 h to the formation of a greater amount of silver nanoparticles, homogeneously nucleated over the surface of bioglass powders. The beaker was kept completely sealed with aluminum foil, as the silver nanoparticles are sensitive to UV radiation. The mixture of thyme extract with the silver nitrate solution, without the addition of bioactive glass, was evaluated by UV-vis (UV-3600 Plus, Shimadzu) to prove the formation of silver nanoparticles. The extract was used as blank and diluted 25 times. The reading was performed from 400 to 700 cm^{-1} after 30 min and 17 h, using a quartz cuvette.

Characterization of bioactive glass containing silver nanoparticles: the powder of bioactive glass was characterized before and after the addition of the nanoparticles for comparison. Fourier transform infrared spectroscopy coupled with attenuated total reflectance (ATR-FTIR, MB-100C26, Boomen) was performed for the evaluation of the formation or alteration of precursor bonds of hydroxyapatite. The spectral range of analysis was from 4000 to 400 cm^{-1} , with a resolution of 4 cm^{-1} and 128 scans. Scanning electron microscopy (SEM, Leo EVO 40 XVP, Carl Zeiss) with energy dispersive spectroscopy (EDS, XFlash 6160, Bruker) was applied to analyze the morphology and verify

the incorporation of silver. For the SEM, the samples were metalized with gold [14].

Antimicrobial properties: the antimicrobial properties of the nanoparticles were evaluated using the disk-diffusion assay on an agar plate. The test was performed using a plate count agar (PCA, Oxoid), brain heart infusion (BHI) broth (Kasvi), and a solution of chloramphenicol 0.5% w/v (Sigma-Aldrich) as the control antibiotic. Briefly, PCA plates were inoculated with a suspension of gram-positive, *Staphylococcus aureus* ATCC 25923 and *Pseudomonas aeruginosa* ATCC 15442, gram-negative, both cultivated at 37 °C/24 h. The bacterial suspension was centrifuged at 10000 g for 5 min at 4 °C, resuspended in saline solution of 0.85% w/v, and standardized on the McFarland scale at 0.5 (10^8 CFU/mL). A standard amount of bioglass with silver nanoparticles (0.01 g) was aseptically deposited on the agar surface. The formation of halos was observed after 24 h of incubation at 37 °C [14].

RESULTS AND DISCUSSION

UV-vis spectroscopy of silver nanoparticles: the pure extract and that with the nanoparticles were diluted 25 times. Without dilution, the formation of nanoparticles leaves the solution with a dark brown color due to the combined vibration of free electrons of the nanoparticles in resonance with light waves, which give rise to a surface plasmonic resonance (SPR) absorption band in the visible region [15]. Thus, UV-vis spectroscopy measures this SPR absorption, and the results are shown in Fig. 1. In the UV-vis spectra, it was possible to observe one peak centered at 433 and 448 nm after 30 min and 17 h, respectively. The wavelength of the absorption peak of the silver nanoparticles resonance is in the range of 400 to 500 nm, which indicates their formation [16]. Furthermore, the frequency and width of optical interaction peaks (SPR) depend on the shape and size of particles

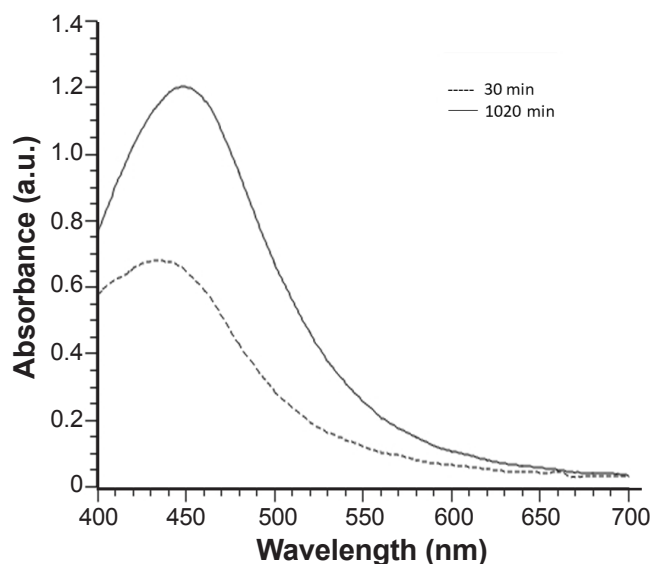


Figure 1: UV-vis spectra from silver nanoparticles after 30 and 1020 min of formation.

[17]. The centering of the peaks at the aforementioned wavelengths implied that the silver nanoparticles were mainly spherical [15, 17]. The increase in peak intensity with the synthesis time indicated an increase in the concentration of the nanoparticles and its shift from 433 to 448 nm was related to an increase in particle size [17]. This was because

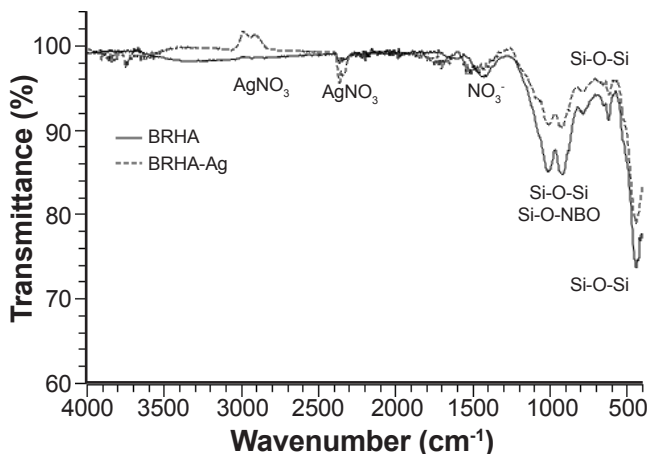


Figure 2: ATR-FTIR spectra for the samples before and after the addition of silver nanoparticles.

the bioreduction of silver ions and their nucleation happened progressively over time and, simultaneously, they grew.

ATR-FTIR: Fig. 2 shows the ATR-FTIR spectra for the samples produced, before and after the addition of silver nanoparticles. The bioactive glass from the rice husk ash (BRHA) before the addition of nanoparticles showed a band at 1428 cm^{-1} , referring to the residual nitrate [18, 19]. Between 760 and 1044 cm^{-1} , it was possible to identify bonds for the groups referring to silica like Si-O-Si that indicated the existence of non-bridging oxygen (NBO) formed by the incorporation of the modifying ions in the silica-forming network. Ca^{2+} and Na^{+} ions break Si-O-Si bonds to form Si-O $^{-}$ species present as SiO $^{-}$ -Ca $^{2+}$ -OSi and SiO $^{-}$ -Na $^{+}$ -OSi [18]. The absorption bands at 916 and 773 cm^{-1} to the BRHA were ascribed to stretching in NBO of Si-O-NBO [18, 20]. The band corresponding to Si-O-Si asymmetrical stretching was located at about 1040 cm^{-1} , while symmetrical stretching was detected at 617 cm^{-1} [19, 20]. The bands between 430 and 511 cm^{-1} were assigned to bending vibrations of Si-O-Si bonds in amorphous silica [20]. These bonds identified for the groups referring to silica (Si-O-Si and Si-O $^{-}$) provide the formation of silanol groups, which is a fundamental step for the growth of the hydroxyapatite layer when the material is

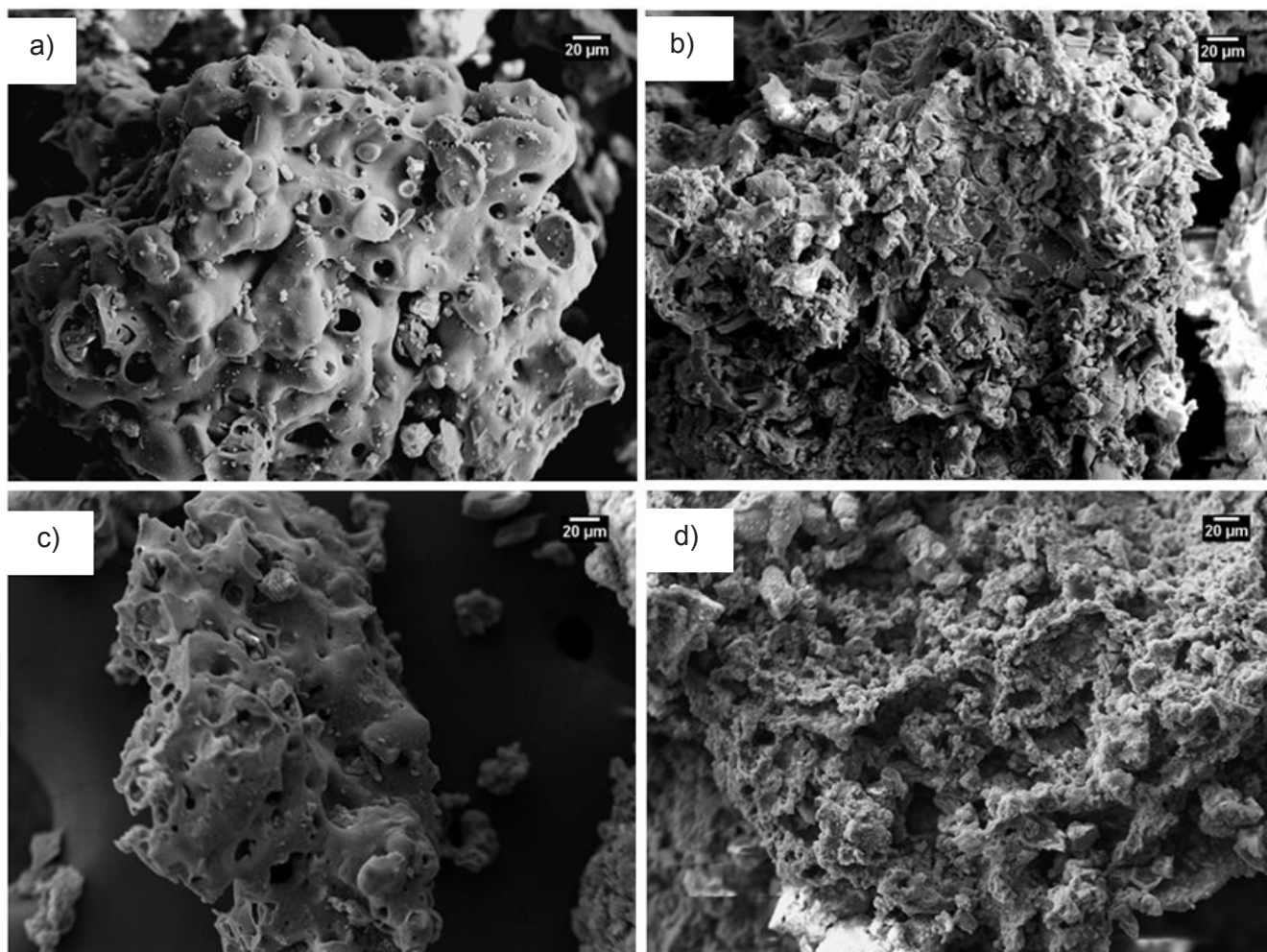


Figure 3: SEM images of the samples before (a,b) and after (c,d) the incorporation of the nanoparticles.

placed in contact with the body fluids [21]. In addition, the interaction verified between the silica and modifying ions indicated the formation of a vitreous network.

The addition of silver nanoparticles did not alter the peaks and, consequently, its relationship with the formation of the hydroxyapatite layer. But new peaks were formed related to the incorporation of the metal in the vitreous network. The

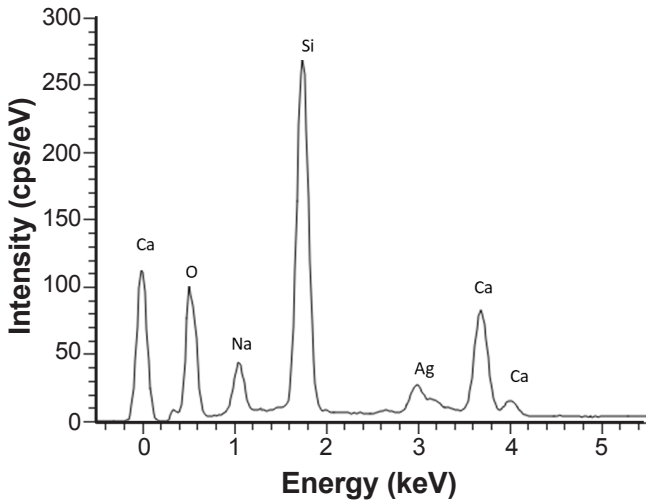


Figure 4: EDS spectrum for the sample after the incorporation of the silver nanoparticles.

peaks at 2355, 2900, and 2980 cm^{-1} are characteristics of the AgNO_3 compound [22]. The possible presence of silver as an Ag^+ ion, in addition to its reduced form, also contributes to its antimicrobial activity [5, 23]. Other characteristic peaks of this molecule were located at 1470 cm^{-1} referring to NO_3^- and 1340, 840, and 810 cm^{-1} , which coincided with those of the bioglass. Thus, the small differences observed in the characteristic peaks of Si-O-Si and NO_3^- bonds demonstrated the interaction between the materials. As the nanoparticles were synthesized by a biogenic route from the thyme extract and there was no heat treatment after incorporation, there could be characteristic bonds of the organic compounds present in the extract, however, these peaks were not observed [16, 24].

Scanning electron microscopy with energy dispersive spectroscopy (SEM-EDS): Fig. 3 shows the scanning electron microscopy images for the samples before and after nanoparticle incorporation. The samples of bioactive glass were formed by a porous agglomerate, which has advantages in drug release [25], for example. Other authors also observed a porous structure of the bioactive material made from rice husks up to a calcination temperature of 1000 $^\circ\text{C}$ [1]. The addition of nanoparticles made the surface rougher, probably due to the deposition of silver. The EDS results proved the incorporation of these nanoparticles into the material, in addition to the presence of the other constituent

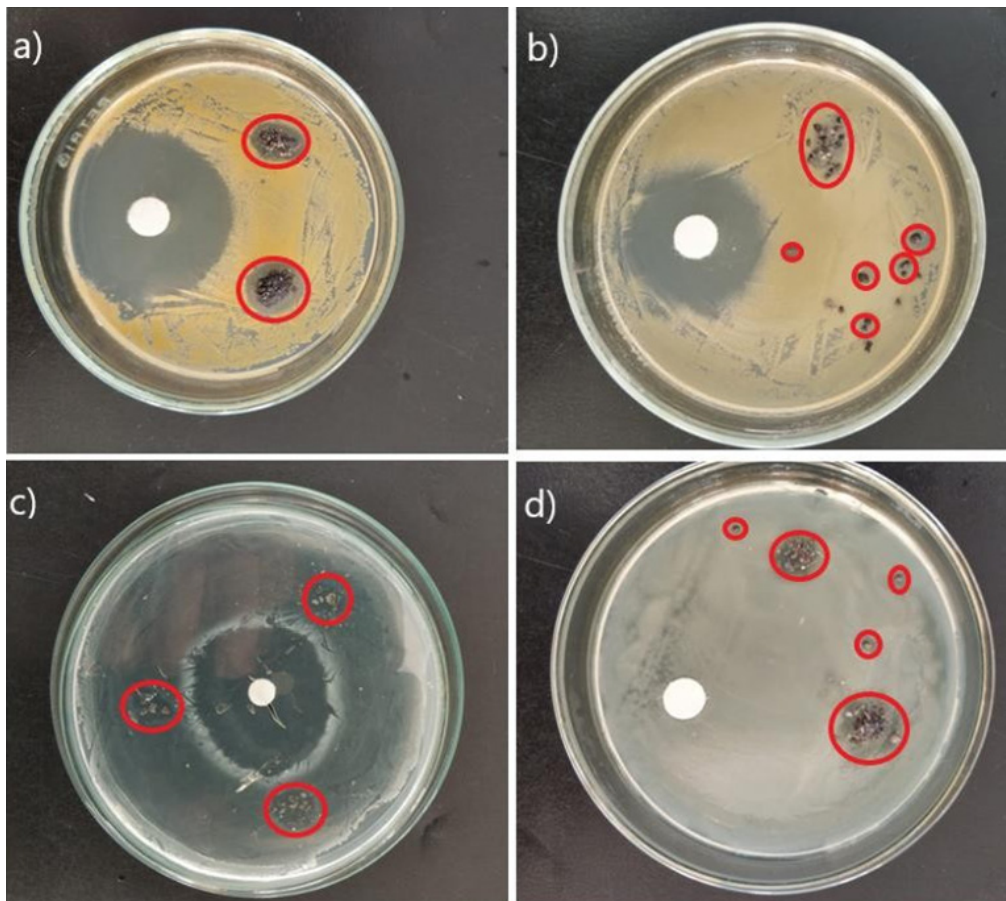


Figure 5: Images of agar diffusion microbiology tests in *S. aureus* (a,b) and *P. aeruginosa* (c,d).

elements of the bioactive glass (Fig. 4). Roughness can imply a greater surface area and, consequently, greater reactivity of the material, which is interesting for this application where ion exchange is desired to form the hydroxyapatite layer and antibacterial action of the Ag⁺ ion.

Antimicrobial properties: microbiological analysis of pure bioactive glass did not inhibit bacterial growth, as verified by other authors [26, 27]. The addition of silver nanoparticles inhibited the growth of both bacteria analyzed, *P. aeruginosa* and *S. aureus* (Fig. 5), which was also observed by other authors by incorporating silver nanoparticles into a vitroceraamic scaffold [27]. The antimicrobial action of nanoparticles occurs through the release of the Ag⁺ ion, but the mechanism of action is still being studied, considering oxidative stress, metal toxicity, and alteration of the permeability of the bacterial cell membrane [28]. The concentration and distribution of the powder were not completely uniform over the plate, which did not allow accurate halo measurements in all samples for a statistical calculation. However, from the measurement of the plaques that presented the best concentration of powder, it was possible to observe an average inhibition zone value of approximately 7 and 8 mm for *P. aeruginosa* and *S. aureus*, respectively. This relatively small zone has also been observed by other authors and is related to the controlled diffusion mechanism of silver that exhibits a reduction in the rate of Ag⁺ release from the vitreous matrix due to the high silver ion electronegativity [14, 29]. The non-uniform dispersion and concentration of particles (Fig. 5) allowed us to infer that regions with fewer particles had smaller halos, that is, the greater the concentration of silver, the greater the inhibitory action [17]. Furthermore, as the powder had dispersion in size, it was possible to observe that the smaller and more dispersed, the greater the inhibition due to the larger contact area created between nanoparticles and microorganisms.

CONCLUSIONS

The synthesis of silver nanoparticles by biogenic route using thyme extract was proven. Its incorporation into the bioglass was verified and did not compromise the initial formation of the vitreous network. Only the surface of the samples became rougher due to the deposition of silver nanoparticles, which can favor the ion exchange necessary for the application of this material. The antimicrobial property of silver nanoparticles was confirmed for two microorganisms, *S. aureus* and *P. aeruginosa*. Thus, this study demonstrated a great potential for the development of a biogenic synthesis route for silver nanoparticles incorporated into a low-cost bioglass for medical applications to reduce the risks of contamination.

ACKNOWLEDGMENT

This work was supported by the National Council for Scientific and Technological Development (CNPq-PVDCF838-2017).

REFERENCES

- [1] J.P. Nayak, J. Bera, *Appl. Surf. Sci.* **257**, 2 (2010) 458.
- [2] N.P. Stochero, E. Marangon, A.S. Nunes, M.D. Tier, *Ceram. Int.* **43**, 16 (2017) 13875.
- [3] Comp. Nac. Abastec., “Acompanhamento da safra brasileira de grãos”, v.1, n.1, CONAB, Brasilia (2021).
- [4] J.A. Santana Costa, C.M. Paranhos, *J. Clean. Prod.* **192** (2018) 688.
- [5] S. Maleki, F. Lot, M. Barzegar-Jalali, *Mater. Sci. Eng. C* **44** (2014) 278.
- [6] S. Ahmed, M. Ahmad, B.L. Swami, S. Ikram, *J. Adv. Res.* **7** (2016) 17.
- [7] H. Duan, D. Wang, Y. Li, *Chem. Soc. Rev.* **44** (2015) 5778.
- [8] P. Singh, Y. Kim, D. Zhang, D. Yang, *Trends Biotechnol.* **34** (2016) 588.
- [9] I.M. Martins, S.N. Rodrigues, M.F. Barreiro, A.E. Rodrigues, *Ind. Eng. Chem. Res.* **50** (2011) 13752.
- [10] R. Gyawali, S.A. Ibrahim, *Food Control* **46** (2014) 412.
- [11] I.M. Martins, S.N. Rodrigues, M.F. Barreiro, A.E. Rodrigues, *Ind. Eng. Chem. Res.* **50** (2011) 898.
- [12] M.A. Pereira, J.E. de Oliveira, C.S. Fonseca, *Cerâmica* **67**, 383 (2021) 333.
- [13] M. Behravan, A. Hossein Panahi, A. Naghizadeh, M. Ziaee, R. Mahdavi, A. Mirzapour, *Int. J. Biol. Macromol.* **124** (2019) 148.
- [14] A.C. Vale, P.R. Pereira, A.M. Barbosa, E. Torrado, N.M. Alves, *Mater. Sci. Eng. C* **94** (2019) 161.
- [15] T.P. Amaladhas, S. Sivagami, T.A. Devi, N. Ananthi, *Adv. Nat. Sci. Nanosci. Nanotechnol.* **3** (2012) 1.
- [16] Y.Y. Mo, Y.K. Tang, S.Y. Wang, J.M. Lin, H.B. Zhang, D.Y. Luo, *Mater. Lett.* **144** (2015) 165.
- [17] J. Huang, G. Zhan, B. Zheng, D. Sun, F. Lu, Y. Lin, H. Chen, Z. Zheng, Y. Zheng, Q. Li, *Ind. Eng. Chem. Res.* **50** (2011) 9095.
- [18] C.A. Bertran, O.V.M. Bueno, *Key Eng. Mater.* **631** (2014) 36.
- [19] H.C. Li, D.G. Wang, C.Z. Chen, *Ceram. Int.* **41**, 8 (2015) 10160.
- [20] S. Palakurthy, K.V. Reddy, S. Patel, P.A. Azeem, *Prog. Biomater.* **9** (2020) 239.
- [21] D. Arcos, D.C. Greenspan, M. Vallet-Regí, *J. Biomed. Mater. Res. A* **65**, 3 (2003) 344.
- [22] NIST Chem. WebBook, “Silver nitrate”, Nat. Inst. Stand. Technol. (2021).
- [23] Z.M. Xiu, J. Ma, P.J.J. Alvarez, *Environ. Sci. Technol.* **45** (2011) 9003.
- [24] J.S. Valli, B. Vaseeharan, *Mater. Lett.* **82** (2012) 171.
- [25] K. Zheng, A.R. Boccaccini, *Adv. Colloid Interface Sci.* **249** (2017) 363.
- [26] C.R. Mariappan, N. Ranga, *Ceram. Int.* **43** (2017) 2196.
- [27] R.L.M.S. Oliveira, L. Barbosa, C.R. Hurtado, L.P. Ramos, T.L.A. Montanheiro, L.D. Oliveira, D.B. Tada, E.S. Trichês, *J. Biomed. Mater. Res. A* **108** (2020) 2447.
- [28] K. Jurczyk, M.M. Kubicka, M. Ratajczak, M.U. Jurczyk, K. Niespodziana, D.M. Nowak, M. Gajecka, M.

Jurczyk, *Trans. Nonferrous Met. Soc. China* **26** (2016) 118.
[29] C. Tanase, L. Berta, A. Mare, A. Man, A.I. Talmaciu,
I. Roşca, E. Mircea, I. Volf, V.I. Popa, *Eur. J. Wood Wood*

Prod. **78** (2020) 281.
(*Rec.* 23/02/2022, *Rev.* 04/03/2022, 25/08/2022, *Ac.*
01/09/2022)

